

Mechanical performance of fiber-reinforced recycled refractory brick concrete exposed to elevated temperatures

Mahdi Nematzadeh* and Ardalan Baradaran-Nasiri^a

Department of Civil Engineering, University of Mazandaran, Babolsar, Iran

(Received January 22, 2019, Revised April 29, 2019, Accepted April 30, 2019)

Abstract. In this paper, the effect of the type and amount of fibers on the physicomaterial properties of concrete containing fine recycled refractory brick (RRB) and natural aggregate subjected to elevated temperatures was investigated. For this purpose, forta-ferro (FF), polypropylene (PP), and polyvinyl alcohol (PVA) fibers with the volume fractions of 0, 0.25, and 0.5%, as well as steel fibers with the volume fractions of 0, 0.75, and 1.5% were used in the concrete containing RRB fine aggregate replacing natural sand by 0 and 100%. In total, 162 concrete specimens from 18 different mix designs were prepared and tested in the temperature groups of 23, 400, and 800°C. After experiencing heat, the concrete properties including the compressive strength, ultrasonic pulse velocity (UPV), weight loss, and surface appearance were evaluated and compared with the corresponding results of the reference (unheated) specimens. The results show that using RRB fine aggregate replacing natural fine aggregate by 100% led to an increase in the concrete compressive strength in almost all the mixes, and only in the PVA-containing mixes a decrease in strength was observed. Furthermore, UPV values at 800°C for all the concrete mixes containing RRB fine aggregate were above those of the natural aggregate concrete specimens. Finally, regarding the compressive strength and UPV results, steel fibers demonstrated a better performance relative to other fiber types.

Keywords: recycled refractory brick; fiber-reinforced concrete; elevated temperatures; ultrasonic pulse velocity; weight loss; mechanical properties

1. Introduction

In recent years, reusing waste materials such as recycled concrete aggregate (RCA) as a partial or total natural aggregates replacement in the production of new concretes has been receiving attention as a commercially acceptable and technically viable method (Sagoe-Crentsil *et al.* 2001). Managing industrial wastes is a serious global challenge of our time, particularly for big cities lacking a landfill (Wijayasundara *et al.* 2018). Recycling non-biodegradable wastes is a difficult practice, and ceramic wastes (with bricks being their subgroup) are classified as this type of wastes with a very long biodegradation period (up to 4000 years); hence, given that a significant share of total industrial ceramic production ends up as waste, recycling ceramic waste has become a major concern (Halicka *et al.* 2013). According to the literature, the first ever case of using crushed brick together with Portland cement was recorded in 1860 Germany to produce concrete products; however, the first case of a significant use of crushed brick as an aggregate in fresh concrete was recorded during the reconstruction efforts after World War II (Hansen 2004).

Among the main benefits of employing crushed refractory brick as an alternative aggregate, enhanced concrete properties after exposure to heat, reduced usage of

natural aggregates, and being regarded as an environment friendly method can be mentioned (Baradaran-Nasiri and Nematzadeh 2017). Moreover, the percentage by which recycled aggregate replaces the natural one affects the stress-strain curve of recycled concretes (Xiao *et al.* 2005). With respect to the study of Liu *et al.* (2016), it can be seen that in the replacement percentage range of 0-100%, the compressive strength and elastic modulus of recycled concretes significantly decreased with increasing temperature, and that the effect of the replacement level of recycled aggregate on the ultimate strain parameter, when the concrete was exposed to heat, was significant, such that as the replacement level increased, so did the concrete ultimate strain. Aliabdo *et al.* (2014) addressed the application of crushed brick in concrete products in their study, in which the compressive strength, porosity, elastic modulus, and ultrasonic pulse velocity (UPV) of the concrete specimens containing 0-100% brick fine and coarse aggregates replacing natural aggregates, as well as their combinations were investigated.

In general, adding fibers in a concrete mixture can improve the mechanical properties of concrete significantly (Yazıcı *et al.* 2007, Afroughsabet *et al.* 2016, Li *et al.* 2017a, Nematzadeh and Fallah-Valukolaee 2017a and b, Domski *et al.* 2017, Ghahremannejad *et al.* 2018). The existence of numerous microcracks throughout concrete volume even before the start of loading prevents a proper transfer of tensile stress during a tension test and proper transfer of tensile strain during a compression test, which in turn lead to further spread of cracks. In addition, application of fibers is recommended for their ability to improve the

*Corresponding author, Associate Professor

E-mail: m.nematzadeh@umz.ac.ir

^aGraduate Student

weakness of concrete in tension and its ductility in compression, as well as give a concrete with fewer cracks, with these improvements depending strongly on the type, shape, and volume fraction of these fibers used in a concrete mix (Soroushian and Bayasi 1991, Poorhosein and Nematzadeh 2018). It can be said that, in general, fibers used in concrete include steel, glass, synthetic, and natural types (Poorhosein and Nematzadeh 2018, Nematzadeh and Hasan-Nattaj 2017). Researchers are still studying the post-cracking behavior of fiber-reinforced concrete (FRC) containing various types of fibers under different loading modes; however, steel and polypropylene (PP) fibers are among those most interesting to the researchers (Choumanidis *et al.* 2016). Buratti *et al.* (2011) demonstrated that steel fibers provide greater stiffness in comparison with macro-synthetic fibers. The effectiveness of steel fibers with different aspect ratios in concrete made with lightweight aggregate was addressed by Güneysi *et al.* (2015).

It is generally believed that the strength deterioration mechanism of concrete under elevated temperatures is attributable to two main factors (Peng *et al.* 2006); 1) an increasing vapor pressure due to moisture evaporation and 2) the formation and propagation of cracks due to thermal stresses, which appear as a result of temperature differences between different parts of concrete (such as surface and core). Since the moisture content and constituents of aggregates are completely different between conventional concrete and concrete with recycled aggregate, the effect of the above two factors must also be different between the two concrete types. Therefore, the performance of recycled aggregate concrete during exposure to heat and after that is of particular interest, which calls for more research (Cree *et al.* 2013). Additionally, the use of fibers in the concrete mix in addition to having benefits such as a low density of some of them including PP and polyvinyl alcohol (PVA) as well as other types of synthetic fibers, and thus a low cost of producing fiber-reinforced concrete (Hsie *et al.* 2008, Yao *et al.* 2003, Qian and Stroeven 2000, Banthia and Gupta 2004), presents higher strength and stiffness values relative to those of conventional concrete even after exposure to elevated temperatures.

Choumanidis *et al.* (2016) examined the effect of different fibers on the flexural behavior of concrete after exposure to heat and showed that steel fibers improved compressive and flexural strengths at ambient temperature and the elevated temperatures and provided a more ductile behavior. Moreover, although polypropylene fibers improved the concrete properties relative to steel fibers at ambient temperature, as the temperature increased, this improvement disappeared. Chen *et al.* (2014) investigated the compressive behavior of FRC containing recycled aggregate after experiencing heat and reported that the compressive strength and elastic modulus of recycled aggregate concrete reinforced with steel fibers showed a small reduction at ambient temperature, while at elevated temperatures, the heated steel fiber-reinforced recycled aggregate concrete demonstrated considerably higher compressive strength and elastic modulus values compared with those of conventional concrete.

The present work was aimed to explore the effect of

Table 1 Characteristics of cement and recycled refractory brick fine aggregate

Composition	Portland cement (CEM-I 42.5N)	Recycled refractory brick
SiO ₂ (%)	20.6	52
Al ₂ O ₃ (%)	4.86	40
Fe ₂ O ₃ (%)	3.37	1.5
CaO (%)	63.56	0.5
MgO (%)	2.18	0.3
Loss on ignition (%)	2.2	-
Refractoriness (°C)	-	1700

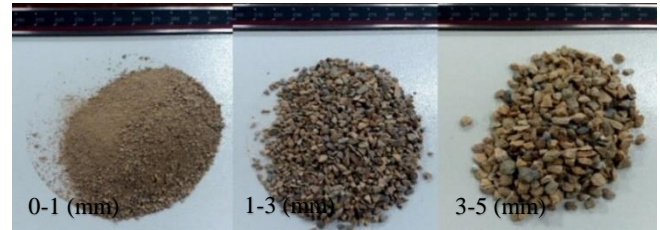


Fig. 1 Different grades of refractory brick aggregate

aggregate type (natural or recycled refractory brick) as well as the type and volume fraction of the fibers used in concrete mix. For this purpose, 162 cubic specimens were prepared using 18 different concrete mixtures in order to investigate the compressive strength, UPV, and weight loss of the concrete specimens at 23, 400, and 800 °C. The fiber types employed here include steel (St), forta-ferro (FF), polypropylene (PP), and polyvinyl alcohol (PVA) fibers, with the volume fraction of 0, 0.25, and 0.5% for FF, PP, and PVA fibers together with 0, 0.75, and 1.5% for St fibers.

2. Experimental study

2.1 Materials

In this study, the materials used in the concrete mix designs included type I Portland cement, recycled refractory brick (RRB) fine aggregate, and natural fine aggregate, as well as St, FF, PP, and PVA fibers, which are described below.

Type I Portland cement (CEM-I 42.5 N) in accordance with the ASTM C150 standard (2003) supplied from a local source was used in all the mix designs of this work. Table 1 shows the properties of this cement.

The concrete prepared in the current work lacked coarse aggregate, thus the fine aggregates used included natural sand and RRB fine aggregate; the former with the fineness modulus, water absorption, specific gravity, and maximum grain size of 2.60, 1.73%, 2.63, and 4.75 mm, respectively. Furthermore, the RRB fine aggregate was used with varying grain size in the range 0.15-4.75 mm, with a grading complying with the ASTM C33 standard (2003). Regarding the tests performed on the crushed bricks, the specific gravity and water absorption were obtained as 2.61 and 2.18%, respectively. Moreover, the properties of refractory brick sand are listed in Table 1, with some photos of

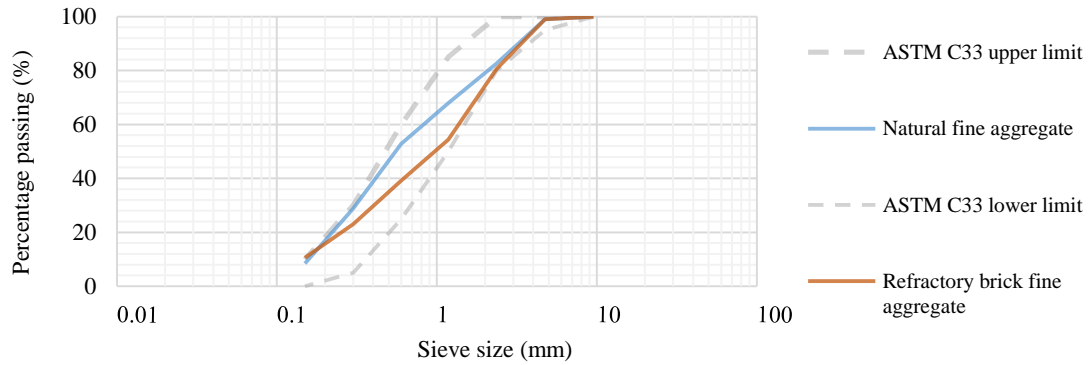


Fig. 2 Gradation curves of natural and recycled refractory brick fine aggregate

Table 2 Properties of different types of fibers

Type of fiber	Shape of fiber	Length (mm)	Diameter (mm)	Aspect ratio l/d	Density (g/cm^3)	Tensile strength (MPa)	Elastic modulus (GPa)	The usual melting point ($^{\circ}C$)
Steel (St)	Crimped and hooked end	25	0.70	36	7.85	1140	200	1370
Polypropylene (PP)	Straight and monofilament	12	0.019	631	0.91	350	3.5	160
Polyvinyl alcohol (PVA)	Straight and monofilament	6	0.011	526	1.3	966	25.5	200
Forta-ferr(FF)	Fibrillated+twisted bundle (Hybrid)	54	0.34	159	0.91	570-660	4.7	160

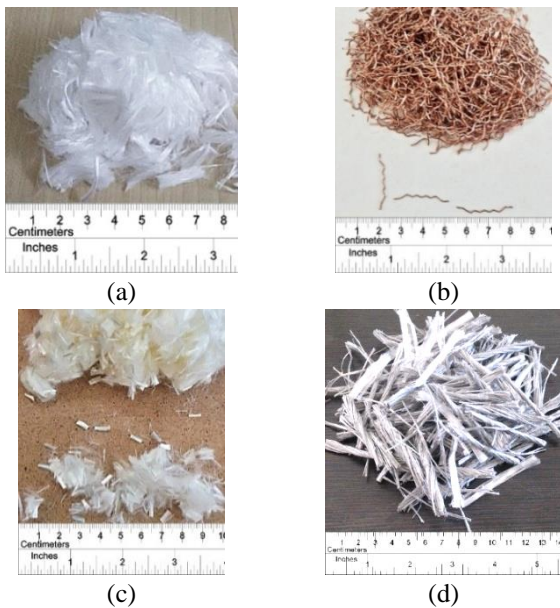


Fig. 3 The shape of different types of fibers used; (a) polypropylene, (b) hooked-end crimped steel, (c) polyvinyl alcohol, and (d) forta-ferro fibers

different grades of RRB fine aggregate given in Fig. 1. In addition, the gradation curves of the natural sand and RRB fine aggregate are demonstrated in Fig. 2.

In this research, PP fibers with the length of 12 mm and aspect ratio (l/d) of 631; PVA fibers with the length of 6 mm and aspect ratio of 526; FF fibers with the length of 54 mm and aspect ratio of 159; as well as hooked-end crimped St fibers with the length of 25 mm and aspect ratio of 36 were used. The geometry and properties of these fibers are given in Fig. 3 and Table 2, respectively. Among these

Table 3 Properties of superplasticizer additive

Form	Aqueous solution of modified poly
Appearance	Viscous liquid
Color	Transparent or milky
Subsidiary effect	Hardening accelerator and high range waer
Solid value	$40 \pm 0.02 \%$
pH	6-8

fibers, FF fibers are considered as more recent, which are consisted of synthetic hybrid fibers made from 100% virgin copolymer/polypropylene in the form of a twisted bundle of non-fibrillated monofilaments together with fibrillated network fibers.

To preserve the workability of concrete and obtain a uniform distribution of fibers in all of the mix designs employed here, a polycarboxylate-based superplasticizer commercially available under the name Carboxal HF5000, containing 40% solid content and having the specific gravity of 1.1 was used as a weight percentage of the cement. Regarding the ASTM C494 standard (2016), this is a type F superplasticizer with properties shown in Table 3.

2.2 Mix proportions

Here, the total of 162 specimens made from 18 different concrete mixes were prepared; among which, a half with different volume fractions of St, FF, PP, and PVA fibers containing RRB fine aggregate (100% of total fine aggregate), and the other half with different volume fractions of the above fibers containing natural fine aggregate (100% of total fine aggregate). The volume fractions of FF, PP, and PVA fibers were considered as 0, 0.25, and 0.5%, while those of the St fibers were regarded

Table 4 Concrete mix proportions

Mix no.	Specimen ID	Fiber V_f (%)	Water-cement ratio (W/C)	SP* (%)	Mix proportions (kg/m ³)				Slump (mm)
					Portland cement	Water	Fine aggregate (SSD**)		
							Conventional	Recycled	
1	Plain-N	0	0.55	0	500	275	1400	0	120
2	FF0.25-N	0.25	0.55	0	500	275	1400	0	125
3	FF0.50-N	0.50	0.55	0	500	275	1400	0	135
4	PP0.25-N	0.25	0.55	2.5	500	275	1400	0	100
5	PP0.50-N	0.50	0.55	5	500	275	1400	0	95
6	PVA0.25-N	0.25	0.55	2.5	500	275	1400	0	105
7	PVA0.50-N	0.50	0.55	5	500	275	1400	0	100
8	St0.75-N	0.75	0.55	1	500	275	1400	0	120
9	St1.50-N	1.50	0.55	2.5	500	275	1400	0	120
10	Plain-R	0	0.55	3	500	275	0	1415	100
11	FF0.25-R	0.25	0.55	2	500	275	0	1415	110
12	FF0.50-R	0.50	0.55	3	500	275	0	1415	115
13	PP0.25-R	0.25	0.55	6.5	500	275	0	1415	90
14	PP0.50-R	0.50	0.55	7	500	275	0	1415	85
15	PVA0.25-R	0.25	0.55	6.5	500	275	0	1415	90
16	PVA0.50-R	0.50	0.55	7	500	275	0	1415	90
17	St0.75-R	0.75	0.55	3.5	500	275	0	1415	100
18	St1.50-R	1.50	0.55	5	500	275	0	1415	100

*Superplasticizer **Saturated surface dry

as 0, 0.75, and 1.5%, respectively. Note that in the existing recommendations, no upper limit is defined for the content of fibers; however, the content of fibers must be maintained at a low level in order to have an adequate workability for the concrete and prevent a heterogeneous distribution of fibers as well as avoid the balling phenomenon.

All the mix designs were considered the same in terms of the water-to-cement ratio (0.55) and the content of fine aggregate; therefore, in the analysis of results, these two were not included as the factors affecting data variations, so as to conduct a more accurate comparison among the effects of fibers on the concrete properties after exposure to elevated temperatures. Details on all the mix designs are presented in Table 4. The negligible difference seen between the contents of fine aggregate used in the recycled concrete mix and in the conventional concrete mix is due to the different specific gravity values of refractory brick sand and natural sand.

The slump value of different mix designs was determined using Abram's cone test in compliance with the ASTM C143/C143M (2003); the results of which are represented in Table 4. In this study, it was attempted to keep the variation of the slump value in a relatively small range for different mix designs by adjusting the dosage of the superplasticizer. Although most studies reported in the literature did not consider the rheological properties (Meng and Khayat 2018), the workability of the FRC mixtures can be affected by fiber content. In fact, adding fibers to concrete mixtures can often increase the surfaces that need to be wetted, so the amount of free water to lubricate cement particles is reduced (Grünwald and Walraven 2001). Since the workability of concrete specimens made from crushed refractory brick aggregate is affected by the water absorption level of the RRB aggregate, it was

moistened up to its water absorption level and kept in the saturated surface dry (SSD) condition for 24 hours prior to preparing the mix design. In addition, since saturating the fine aggregate in the water tank then drying their surface is not as easy as it is for the coarse aggregate, the RRB fine aggregate was placed in plastic bags, and the water required for saturation was poured in them, then by shaking the bags, water was properly mixed with the aggregate grains before the mixture was left for 24 hours; finally, it was used to make the concrete specimens. This method had previously become common practice by Khalaf *et al.* (2004, 2005).

The IDs given to the concrete specimens and mixes are given in Table 4, in which it is seen that apart from the specimens without any fiber, the IDs assigned to each group of mix designs consist of three parts; the first letters specify the fiber type, with the following numbers indicating the volume fraction of fibers used, and at the end of IDs, the letter N and R represent natural and RRB fine aggregates, respectively. For example, FF0.25-R represents a specimen containing 0.25% FF fibers with 100% RRB fine aggregate. Furthermore, for the specimens without any fiber, Plain-N and Plain-R indicate the specimens containing 100% natural fine aggregate and 100% RRB fine aggregate, respectively.

2.3 Specimen preparation

In order to prepare a concrete mix, first the aggregate and cement were mixed in the dry state for 1 min, then water and the superplasticizer were gradually added to the original mix, and the mixing procedure continued for 2 min. In the next stage, fibers were added in the resulting mix, and the mixing continued for another 3 min. At this point, the fibers were adequately dispersed throughout the mix to prevent the balling of the fibers while mixing.

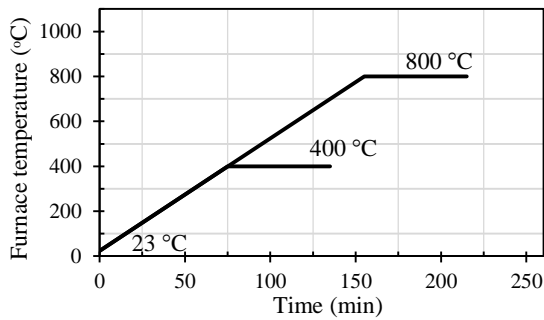


Fig. 4 Heating regimes inside the electric furnace for concrete specimens

Subsequently, the fresh concrete mixes were cast into cubic $100 \times 100 \times 100$ mm molds. To minimize experimental errors, for each mix design and temperature applied to the specimens, three identical cubic specimens were made. Unmolding the specimens was carried out 24 h after casting the concrete, and then, the specimens were cured in a tank with water at 23°C and the moisture level of 100% for 28 days in compliance with the ASTM C192 specifications (2002). In the next stage, the cured specimens were removed from the water tank to be air-dried at the ambient environment of the laboratory for 6 days, then those specimens which were to undergo elevated temperatures were placed under the temperature of 110°C for 24 h in an oven to get oven-dried before being put into the furnace. Finally, this group of specimens were exposed to the temperatures of 400 and 800°C and subjected to compressive strength, weight loss, and UPV tests along with the unheated specimens, after cooling and reaching the ambient temperature.

2.4 Thermal treatment

Each group of the concrete specimens was investigated in three thermal series, namely 23, 400, and 800°C . 23°C was considered as the ambient (reference) temperature, and the other two temperatures were regarded as the elevated temperatures to examine the concrete properties after exposure to elevated temperatures. To experience the elevated temperatures, the selected specimens were placed in a vertical $800 \times 800 \times 800$ mm electrical furnace and kept under the target temperatures for 1 h after reaching them in

the furnace (Baradaran-Nasiri and Nematzadeh 2017, Ariozi 2007, Mohammadhosseini and Yatim 2017, Sarhat and Sherwood 2012, Nematzadeh and Baradaran-Nasiri 2018). The internal temperature of the furnace was adjustable and could be read via internal thermocouples. The thermal loading rate was considered as $5^\circ\text{C}/\text{min}$ in this research, with the heating regime applied given in Fig. 4. After thermal loading, the specimens were left in the furnace to reach ambient temperature. Immediately after reaching this temperature, the specimens went through compressive loading and other tests. It is worth noting that all the specimens subjected to 400 and 800°C had already experienced the temperature of 110°C (oven temperature).

2.5 Experiments on hardened concrete

In order to evaluate and compare the concrete specimens after thermal treatment, physicomaterial properties including the compressive strength, UPV, and weight loss of the specimens were determined at different temperatures. Moreover, the changes appeared on the surface of the specimens after exposure to the elevated temperatures were inspected visually.

The compressive strength testing of the specimens was performed based on the BS 1881-116 standard, in which axial loading was applied on the heated concrete specimens immediately after reaching ambient temperature using a 200-ton hydraulic jack. A constant compressive loading rate equal to $0.25 \text{ MPa}/\text{s}$ was considered, which is in compliance with the specified standard range ($0.2\text{--}0.4 \text{ MPa}/\text{s}$).

Based on the ASTM C597 (2016), the nondestructive ultrasonic pulse velocity (UPV) test was conducted on the cubic specimens after a curing period of least 28 days and before conducting the compressive strength test. In this test, the transmission velocity of an ultrasonic pulse is determined via the Direct Transmission method being more precise than the two other methods stated in the ACI 228.2R code (Indirect and Semi-direct). This test was carried out using a portable ultrasonic nondestructive digital indicating tester (PUNDIT, Model PC 1012), with the reported results being the average of the results of similar specimens. In all the experiments, to ensure a proper contact between the specimen surface and the transducers and to facilitate the ultrasonic energy transfer from the transducers to the test specimen, a thin layer of couplant (refractory grease) was applied to the specimen surface.

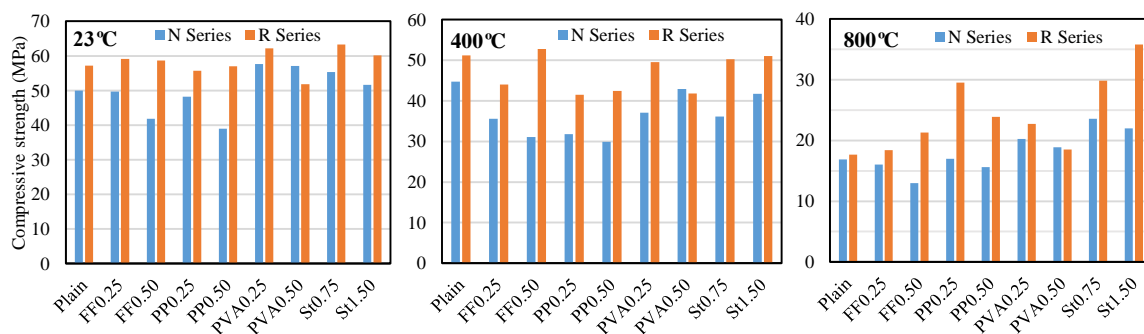
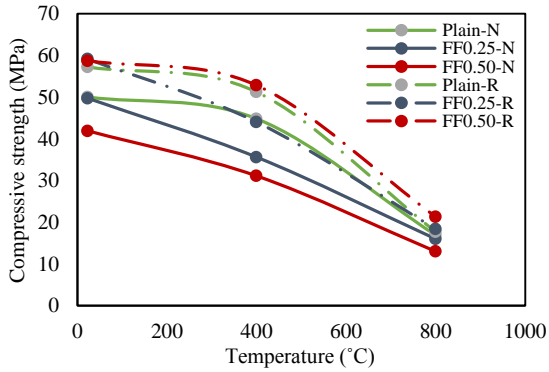
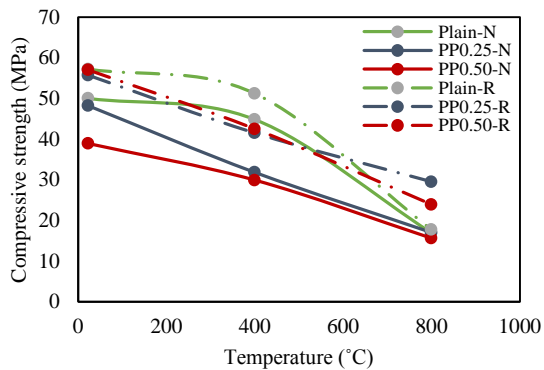


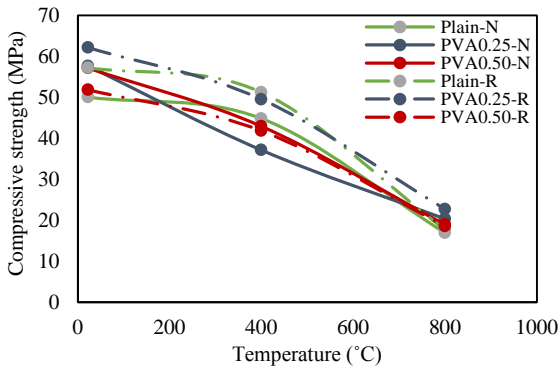
Fig. 5 Effect of different types of fine aggregate on compressive strength in each thermal group



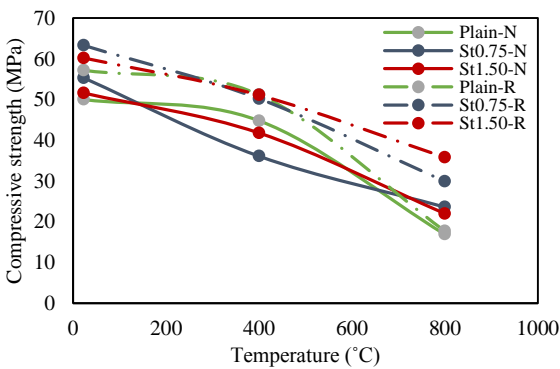
(a)



(b)



(c)



(d)

Fig. 6 Effect of different types of fibers on compressive strength; (a) forta-ferro, (b) polypropylene, (c) polyvinyl alcohol, and (d) steel fibers

3. Results and discussion

Table 5 Compressive strength test results

Mix no.	Specimen ID	23°C		400°C		800°C	
		Mean in MPa	COV (%)	Mean in MPa	COV (%)	Mean in MPa	COV (%)
1	Plain-N	50	4.2	44.8	0.9	16.9	6.2
2	FF0.25-N	49.7	2.1	35.6	6.6	16	3.7
3	FF0.50-N	41.9	2.6	31.1	7.7	13	5.1
4	PP0.25-N	48.2	4.2	31.8	9.3	17	8.5
5	PP0.50-N	38.9	3.7	29.9	9.1	15.6	7.3
6	PVA0.25-N	57.6	0.5	37.1	6.6	20.3	8.7
7	PVA0.50-N	57.1	0.7	42.9	9.1	18.9	8.6
8	St0.75-N	55.3	0.8	36.1	8.8	23.6	5.2
9	St1.50-N	51.6	9.2	41.8	7.2	22	8.7
10	Plain-R	57.2	0.6	51.2	4.6	17.7	3.9
11	FF0.25-R	59.1	1.6	44	8.4	18.4	4.6
12	FF0.50-R	58.7	2.5	52.8	6.3	21.3	9.3
13	PP0.25-R	55.7	3.3	41.5	9.4	29.5	3.4
14	PP0.50-R	57	1.6	42.5	7.3	23.9	5.7
15	PVA0.25-R	62.1	0.1	49.5	6.1	22.7	6.9
16	PVA0.50-R	51.8	2.2	41.8	7.6	18.5	1.1
17	St0.75-R	63.3	1.9	50.2	6.8	29.9	6.9
18	St1.50-R	60.2	6.1	51.1	5.3	35.8	4.3

3.1 Compressive strength

The average values of compressive strength for all the concrete groups made with RRB or natural fine aggregate and containing St, FF, PP, and PVA fibers are demonstrated in Figs. 5 and 6. Furthermore, the compressive strength values together with the coefficient of variation (COV) of each specimen are listed in Table 5. Note that based on the results, at ambient temperature, the highest and lowest average compressive strength values belong to the St0.75-R and PP0.50-N mixes being 63.3 and 38.9 MPa, respectively. As can be observed in Fig. 5, using 100% RRB fine aggregate led to an increase of the compressive strength in almost all the mixes, with the exception of the PVA0.50 mix for which a 9.2% decrease was obtained for the compressive strength of the specimen with RRB fine aggregate relative to that of the one with natural fine aggregate. In general, at ambient temperature, the highest compressive strength increase values due to RRB fine aggregate replacement were seen in the specimens PP0.50 and FF0.50 as 46.5 and 40.1%, respectively, suggesting a better performance of the volume fraction of 0.5% of either fiber type (PP or FF) when used in parallel with RRB fine aggregate. Also, for the conventional (without any fiber) concrete mixes, substitution of RRB fine aggregate resulted in a 14.4% increase of the compressive strength in comparison with that of the corresponding specimen containing natural fine aggregate.

At 400°C, the average compressive strength of all the concrete mixes decreased given the high temperature they experienced. At this temperature, with regard to the results presented in Table 5, the highest and lowest average compressive strength values in the RRB fine aggregate-containing groups belong to the FF0.50 and PP0.25 mixes as 52.8 and 41.5 MPa, respectively. Additionally, in the

natural fine aggregate-containing groups, these two extremes of average compressive strength belong to the Plain and PP0.50 mixes as 44.8 and 29.9 MPa, respectively. Furthermore, it is also seen in Fig. 5 that using 100% RRB fine aggregate resulted in a higher concrete compressive strength in all the mixes containing it, with the only exception being the PVA0.50 mix showing about 2.6% reduction of the compressive strength relative to that of the corresponding natural fine aggregate-containing specimen. Altogether, at 400°C, the greatest compressive strength increase values due to RRB fine aggregate replacement belong to the specimens FF0.50 and PP0.50 as 69.7 and 42.1%, respectively, emphasizing a better performance of using either PP or FF fiber types at the volume fraction of 0.5% along with RRB fine aggregate. Moreover, for the conventional (without any fiber) concrete mixes, the replacement of RRB fine aggregate gave a 14.3% improvement of the compressive strength compared with that of the corresponding natural fine aggregate-containing mixes.

As the temperature raised again to reach 800 °C, average compressive strength values for all the concrete mixes further decreased, with a reduction rate greater than that at 400°C for most specimens. Regarding the results presented in Table 5, the highest and lowest compressive strength values at 800°C in the groups containing RRB fine aggregate pertain to the St1.50 and FF0.25 mixes as 35.8 and 18.4 MPa, respectively. In addition, in the natural fine aggregate-containing groups, these values pertain to the St0.75 and FF0.50 mixes being 23.6 and 13 MPa, respectively. As can be seen in Fig. 5, using 100% RRB fine aggregate replacing natural fine aggregate increased the compressive strength in all the associated concrete mixes, and similar to the other temperatures, only for the PVA0.50 mix, a 2.1% decrease of the compressive strength was observed for the specimen with RRB fine aggregate compared with the one with natural fine aggregate. In general, at 800°C, the greatest compressive strength improvement due to RRB replacement belonged to the specimen PP0.25 with 73.5%; however, the significant improvement of the compressive strength for the specimens FF0.50 and PP0.50 with 63.8 and 53.2% increase, respectively, proves an acceptable performance of PP and FF fibers at the volume fraction of 0.5% along with RRB fine aggregate. Furthermore, for the conventional (without any fiber) mixes, the substitution of RRB fine aggregate led to a 4.7% compressive strength improvement relative to that of the corresponding specimens containing natural fine aggregate.

Altogether, with respect to the above results, it can be said that the usage of RRB fine aggregate as a natural fine aggregate replacement for concretes exposed to heat was very effective (except PVA0.50 mix), with 4 out to 18 mixes showing compressive strength improvements of more than 50% at 800°C. According to the details given in Table 1, the refractory brick used in this article has refractoriness level of about 1700°C and maintains its physical consistency and integration at elevated temperatures; therefore, it can be expected that by applying this or similar materials, concrete with high resistance to heat can be produced.

For all the concrete mixes, the coefficient of variation (COV) of compressive strength was determined to be less than 10% and varying in the range 0.1-9.4% for different temperature groups, as can be seen in Table 5.

The effect of individual fiber types on the concrete compressive strength is presented in Fig. 6. As can be seen in Fig. 6a, using FF fibers at the volume fraction of 0.50% along with RRB fine aggregate demonstrates a better performance relative to that at the volume fraction of 0.25% for all the temperatures, while this is not case for using this fiber type along with natural fine aggregate, and the volume fraction of 0.25% gives a higher compressive strength. With increasing temperature and at 800°C, the compressive strength reduction range for all the FF fiber-containing mixes is from 64 to 69%, indicating that the performances of these specimens under elevated temperatures are almost similar.

With respect to Fig. 6(b), using the 0.50% volume fraction of PP fibers together with RRB fine aggregate shows a better thermal performance relative that of the 0.25% volume fraction up to 400°C, while this is not the case when using this fiber type with natural fine aggregate, and the volume fraction of 0.25% gives a higher compressive strength at all the temperatures. Moreover, regarding the figure it is safe to say that adding PP fibers in the concrete mix improves compressive strength under even higher temperatures (800°C), thus employing this fiber type is recommended for concrete specimens. Improved performance when using PP fibers in concrete under elevated temperatures, as discussed by Mohammadhosseini *et al.* (2018), can be attributed to the creation of networks after the melting of the fibers, which results in the release of the induced thermal pressure and pore pressure. It should also be noted that the melting of fibers and the creation of space for the release of the pore water pressure prevents further loss of concrete strength (Mohammadhosseini and Yatim 2017). As the temperature increased and at 800°C, the compressive strength reduction range for the mixes containing PP fibers was 47-65%, with the best performance pertaining to PP0.25-R which showed a strength of 29.5 MPa by maintaining 47% of its original strength.

Regarding Fig. 6(c), using the 0.50% volume fraction of the PVA fibers along with both types of fine aggregate shows a weaker thermal behavior in comparison with that for the 0.25 volume fraction at all the test temperatures (except at 400°C for natural fine aggregate-containing concrete). In fact, increasing the content of PVA fibers did not improve the compressive strength, and contrary to the expectation that it would show a better behavior than PP fibers, no acceptable performance was achieved for PVA fibers. This may be a consequence of the improper distribution of high contents of this fiber type throughout the concrete mix, which resulted in a weaker performance in comparison with that of its lower contents. With increasing temperature and at 800°C, a compressive strength loss range of 63-67% was achieved for the mixes with PVA fibers, which indicates that the compressive behavior of these fibers, when used along with RRB fine aggregate, is poorer than that of PP fibers at 800°C.

It is seen in Fig. 6(d) that using the hooked end crimped

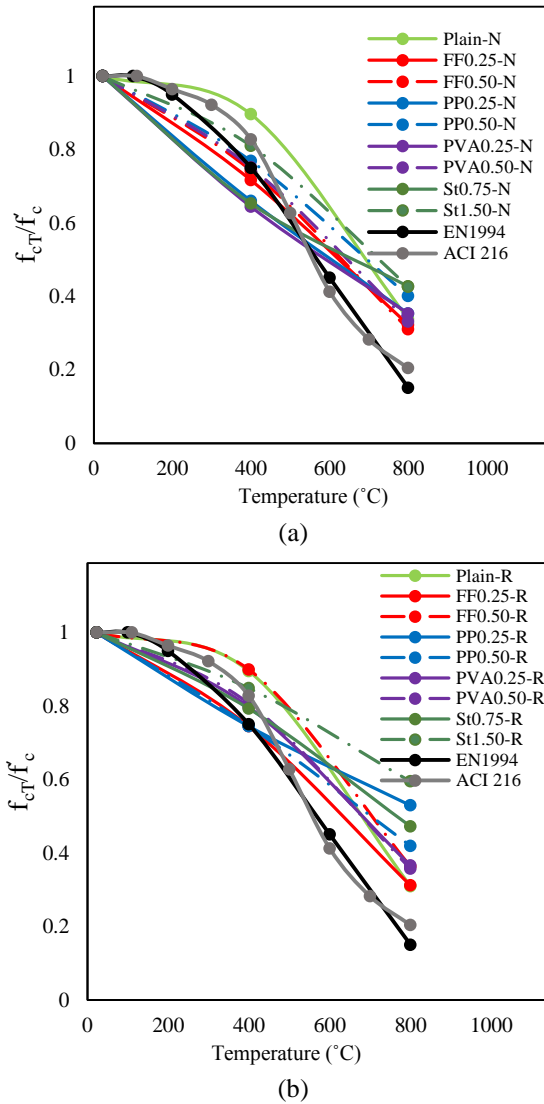


Fig. 7 Normalized compressive strength of concrete as a function of temperature; (a) mixtures containing natural fine aggregate and (b) mixtures containing RRB fine aggregate

steel (St) fibers at the volume fraction of 0.75% together with both the fine aggregates gave a higher compressive strength in comparison with that of the volume fraction of 1.5% at ambient temperature. With increasing temperature, as can be seen, the compressive strength reduction compared with the reference (unheated) value for the concrete containing this fiber type is smaller relative to that of the other fiber types; hence, it can be concluded that employing steel fibers enhances the concrete thermal behavior, in particular at 800°C. As the temperature further raised to reach 800°C, the compressive strength loss of the St fiber-containing mixes varied from 40 to 57%, with the best performance for the St1.50-R specimen showing a 35.8 MPa strength while preserving about 40% of its original strength.

Altogether, to conduct a general comparison among the fiber-reinforced mixes, it can be stated that as the temperature raised to 400°C, the lowest average strength loss (average of loss results for 4 types of fiber-reinforced

concrete mixes made for each fiber type) belongs to the St fibers with 22.4%, and above 400 and up to 800°C, the lowest average strength loss still belongs to the St fibers with 38.1%. Therefore, it is safe to say that among the fibers used in this study, the St fibers demonstrated the best performance in terms of preserving the compressive strength of concrete exposed to heat. The next places in terms of the lowest average compressive strength loss and heating performance level were taken by PP, PVA, and FF fibers in a descending order; however, the FF fibers with the average loss of 22.4% at 400°C reached a value close to that of the St fibers and demonstrated a better performance relative to the other fiber types at this temperature.

The normalized compressive strength for siliceous aggregate concretes as a function of temperature, proposed by the EN 1994-1-2 and ACI 216 codes, is shown in Fig. 7. Note that the curves presented by the EN 1994-1-2 in Fig. 7 refer to those heated concretes cooled at ambient temperature, thus they are different from the curves proposed by EN-1992-1-2 for heated concrete without cooling.

It is also observed in Fig. 7 that the experimental results of the concrete specimens containing natural fine aggregate are closer to the curves proposed by the two above codes than those of RRB fine aggregate-containing specimens. As can be seen in Fig. 7(a), the equation developed by the EN 1994-1-2 overestimates the experimental results of the normalized compressive strength of all the mixes containing natural fine aggregate at temperatures lower than around 200°C (except the concrete without any fiber, the result of which almost conforms to EN 1994-1-2), and with increasing temperature up to around 400°C, it is seen that the experimental results of the fiber-reinforced mixes, particularly higher volume fractions in each fiber group, get considerably close to the values proposed by the EN 1994-1-2. However, at even higher temperatures of about 550°C, the values proposed by the EN 1994-1-2 underestimate the experimental values of all the concrete mixes. In addition, an overestimation for the predictions of the ACI 216 regarding the experimental results of the normalized compressive strength of the natural fine aggregate-containing specimens (except the specimen without any fiber) is observed up to around 400°C, while above that up to around 550°C, the predicted and experimental curves get close to each other, and then, an underestimation is obtained for all the mixes (including the mix without any fiber) by this code, similar to the case for the EN 1994-1-2. For the specimens containing RRB fine aggregate, as can be seen in Fig. 7(b), the predictions provided by the two codes of EN 1994-1-2 and ACI 216 are close to the experimental results at temperatures below 400°C, and beyond the temperature of around 550°C, they are considerably higher than the experimental results. It is worth mentioning that according to Fig. 7, the distribution and scattering of the normalized compressive strength results for the specimens containing RRB fine aggregate at 800°C is greater than that of the natural fine aggregate-containing concrete.

By applying the nonlinear regression analysis of the experimental results, the relationship of the normalized compressive strength (f_{cr}/f_c) with the parameters of temperature (T) and fiber volume fraction (V_f) for the mixes

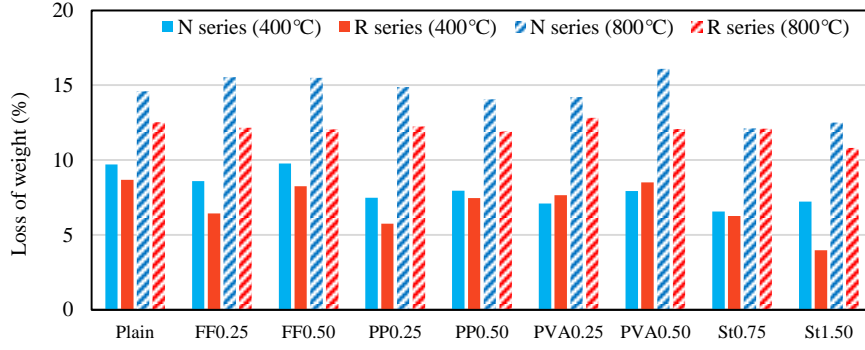


Fig. 8 Weight loss of mixtures exposed to elevated temperatures

containing polymeric fibers, i.e., FF, PP, and PVA fibers, together with natural or RRB fine aggregate is expressed as Eq. (1). The parameters α and β in the equation depend on the fiber volume fraction and temperature, respectively, which are defined for the natural fine aggregate-containing group as α_N and β_N ; and for the RRB fine aggregate-containing group as α_R and β_R . The coefficient of determination (R^2) of this equation is calculated as 0.93 and 0.88 for the mixes containing natural and RRB fine aggregate, respectively, suggesting a good regression of the experimental results.

With regard to the difference between the thermal performance of steel fibers and that of the polymeric fibers, by employing the nonlinear regression analysis, the relationship of the normalized compressive strength (f_{cT}/f'_c) with the parameters of temperature (T) and fiber volume fraction (V_F) for the mixes containing this fiber type along with natural or RRB fine aggregate is expressed as Eq. (2). As described for the polymeric fibers, here, the parameters α and β are also defined for the natural fine aggregate group as α_N and β_N ; and for the RRB fine aggregate group as α_R and β_R , for which the associated formulas are given in Eq. (2). The coefficient of determination (R^2) is 0.89 and 0.82 for the mixes containing natural and RRB fine aggregate, again suggesting a good regression for the experimental results.

$$\text{FF, PP, PVA fibers: } \begin{cases} \frac{f_{cT}}{f'_c} = \alpha/1 + e^\beta \\ \alpha_N = -0.38V_F^2 + 0.1V_F + 1.13 \\ \beta_N = -1.9 + 0.0033T \\ \alpha_R = -0.38V_F^2 + 0.1V_F + 1.1 \\ \beta_R = -2.9 + 0.0047T \end{cases} \quad (1)$$

$$23^\circ\text{C} \leq T \leq 800^\circ\text{C}$$

$$0 \leq V_F \leq 0.5$$

$$\text{Steel fibers: } \begin{cases} \frac{f_{cT}}{f'_c} = \alpha/1 + e^\beta \\ \alpha_N = 0.09V_F^2 - 0.02V_F + 1.08 \\ \beta_N = -2 + 0.003T \\ \alpha_R = 0.12V_F^2 - 0.02V_F + 1.08 \\ \beta_R = -2 + 0.0033T \end{cases} \quad (2)$$

$$23^\circ\text{C} \leq T \leq 800^\circ\text{C}$$

$$0 \leq V_F \leq 1.5$$

In the above equations, f'_c and f_{cT} are the compressive strength of each concrete mix at ambient temperature and elevated temperatures, respectively.

3.2 Weight loss

The weight of specimens before and after exposure to heat was measured to assess the weight loss of each group of the concrete specimens. The weight variations of different concrete specimens at 400 and 800°C relative to that at ambient (reference) temperature are presented in Fig. 8. In general, the amount of weight loss for all the concrete mixes increases with increasing temperature, which is attributed to factors such as the loss of free water and chemical composition water. The experimental results obtained here indicated that at 400°C, using 100% RRB fine aggregate as natural fine aggregate replacement led to a weight loss decrease of the concrete specimens (except for PVA fiber-containing mixes) and a positive effect on preserving the concrete integrity. Furthermore, the weight loss range of all the specimens containing natural fine aggregate at 400°C was between 6.57 and 9.77%, with the minimum and maximum values pertaining to the St0.75 and FF0.50 mixes, respectively. The corresponding range for the RRB fine aggregate-containing specimens was 3.98–8.68%, with the minimum and maximum values pertaining to the St1.50 and Plain mixes, respectively.

As can be seen in Fig. 8, at 800°C, the specimens containing RRB fine aggregate show a lower weight loss in comparison with that of the specimens containing natural fine aggregate, suggesting that using 100% RRB fine aggregate as a natural fine aggregate replacement results in a reduced weight loss of the concrete specimens and has a positive effect on preserving the durability of concrete, similar to the results obtained for 400°C. For further clarification, the weight loss range of the specimens containing natural fine aggregate is 12.11–16.10%, with the lowest and highest values pertaining to the St0.75 and PVA0.5 mixes, respectively. Moreover, this range is 10.82–12.82% for the RRB fine aggregate-containing specimens, with the lowest and highest values for the St1.50 and PVA0.25 mixes, respectively.

Fig. 8 also demonstrates the effect of the type and volume fraction of fibers in the concrete mixes on their weight loss level. As can be seen, employing the 0.25% volume fraction of FF fibers has a better performance than

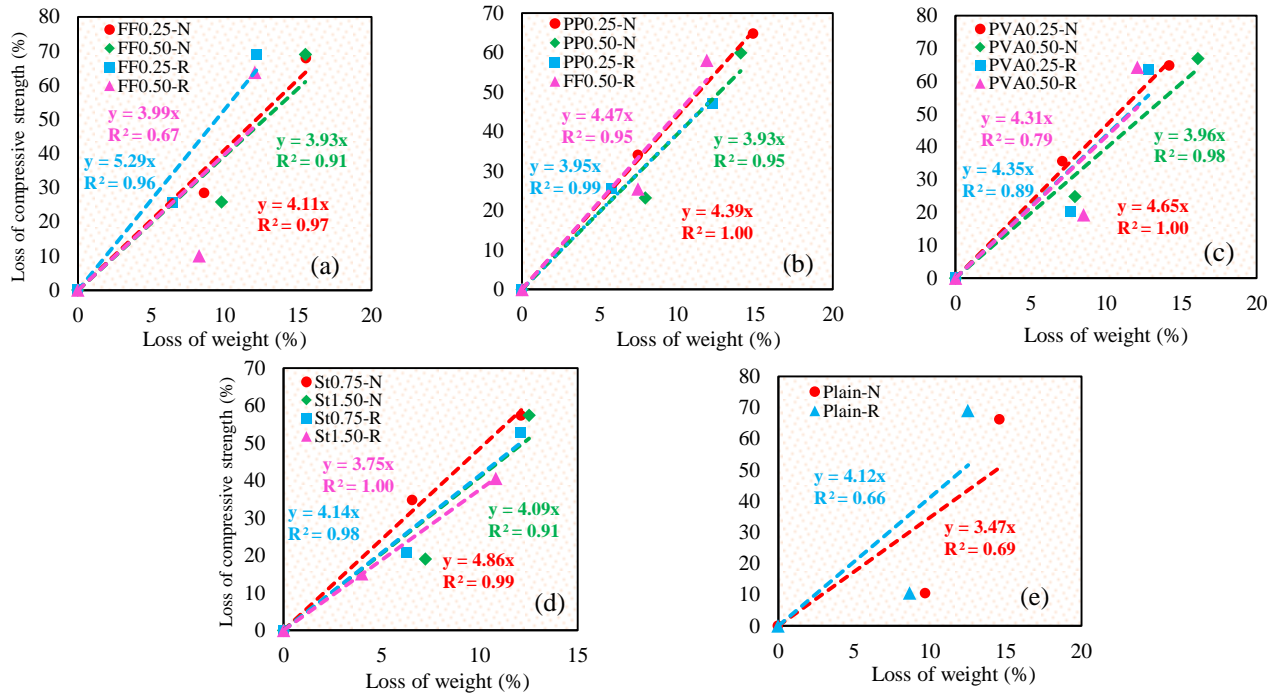


Fig. 9 Relationships between weight loss and compressive strength loss of mixtures; (a) forta-ferro, (b) polypropylene, (c) polyvinyl alcohol, (d) steel fibers, and (e) plain

the 0.5% volume fraction (for both types of fine aggregate) at 400°C, while at 800°C, using different volume fractions of this fiber type shows a negligible effect on weight loss. In addition, for either fine aggregate type, using PP fibers at the volume fraction of 0.25% gives lower weight loss values compared with those at the volume fraction of 0.5%, while a different trend is observed as the temperature raised to 800°C, where a lower volume fraction gives a higher weight loss.

Moreover, at 400°C, the application of PVA fibers at the volume fraction of 0.25% gives a lower weight loss than that at the volume fraction of 0.5% for either fine aggregate type; however, as the temperature increases to 800°C, a lower volume fraction results in a higher weight loss for the mixes containing RRB fine aggregate, while for the natural fine aggregate, a higher volume fraction still gives a higher weight loss. The reason underlying higher weight loss values for higher volume fractions of the polymeric fibers may be that as the temperature increases and these fibers melt as a consequence, the melted fibers together with the water vapor produced from the cement paste dehydration escape from the specimens through the cracks appeared within the concrete. In the end, it can be said that similar to what was previously observed for the compressive strength, the best thermal behavior here also belongs to the St fiber-reinforced mixes, indicating the excellent performance of these fibers. Note that the steel fibers at the volume fraction of 0.75% yielded almost similar values for both types of fine aggregate, while using the St fibers at the volume fraction of 1.5% together with RRB fine aggregate exhibited the best performance among the 18 mixes, with the lowest weight loss.

3.3 Weight loss-compressive strength loss relationship

The diagrams given in Fig. 9 show the weight loss-compressive strength loss relationships of the concrete mixes. With respect to the figure, there is a linear relationship between the weight loss and compressive strength loss. By applying the linear regression analysis on the experimental results of the two parameters, linear equations were developed for the specimens without any fiber and specimens containing St, FF, PP, and PVA fibers, which have high coefficients of determination. From the regression lines obtained in Fig. 9, it is seen that the compressive strength loss of these mixes varies in the range of 3.47-5.29 times as much as their weight loss. It is also found from these results that regarding the FF fibers, using the volume fraction of 0.5% decreases the slope of the weight loss-compressive strength loss relationship relative to that when using the volume fraction of 0.25%, and that for these fibers, using natural fine aggregate relative to RRB fine aggregate provides a smaller diagram slope. In addition, regarding Fig. 9(b), a different trend of the weight loss-compressive strength loss relationship is observed for each fine aggregate type, such that in case of natural fine aggregate, the relationship slope decreases with increasing content of PP fibers, while for RRB fine aggregate, an increase is seen in the slope of the existing relationship with increasing fiber content. Note that reduction of the relationship slope is considered as the desired behavior, which indicates a mix with a higher preserved compressive strength while losing its weight.

Figs. 9(c) and 9(d) demonstrate the weight loss-compressive strength loss relationships for the PVA and St fibers, respectively, according to which, using natural fine aggregate or RRB fine aggregate gives the same trend for the weight loss-compressive strength loss relationship, with a decreasing relationship slope with an increasing volume

Table 6 Ultrasonic pulse velocity test results

Mix no.	Specimen ID	23°C			400°C			800°C		
		Mean in (km/s)	COV (%)	Q*	Mean in (km/s)	COV (%)	Q*	Mean in (km/s)	COV (%)	Q*
1	Plain-N	4.10	1.03	G	3.35	1.09	M	2.04	2.63	P
2	FF0.25-N	4.09	1.91	G	3.20	6.11	M	1.99	0.74	P
3	FF0.50-N	3.95	3.56	G	2.97	2.50	P	1.86	2.93	P
4	PP0.25-N	4.01	2.75	G	3.20	7.20	M	2.06	5.70	P
5	PP0.50-N	4.01	1.59	G	3.20	3.22	M	1.95	2.20	P
6	PVA0.25-N	3.99	5.06	G	3.32	2.78	M	2.08	4.50	P
7	PVA0.50-N	4.18	0.26	G	3.42	4.37	M	2.09	1.66	P
8	St0.75-N	4.16	1.29	G	3.39	5.02	M	2.22	3.59	P
9	St1.50-N	4.02	3.04	G	3.36	4.05	M	2.17	4.27	P
10	Plain-R	4.21	0.70	G	3.27	3.55	M	2.19	1.60	P
11	FF0.25-R	3.91	2.41	G	3.37	3.02	M	2.32	2.44	P
12	FF0.50-R	4.23	0.60	G	2.88	0.49	P	2.25	3.64	P
13	PP0.25-R	4.10	3.27	G	3.40	8.55	M	2.64	3.83	P
14	PP0.50-R	3.72	1.75	G	3.17	4.54	M	2.36	4.27	P
15	PVA0.25-R	4.18	1.72	G	3.14	6.45	M	2.40	2.48	P
16	PVA0.50-R	4.08	4.32	G	3.23	6.71	M	2.25	2.00	P
17	St0.75-R	4.11	2.77	G	3.72	0.35	G	2.50	0.58	P
18	St1.50-R	4.04	2.12	G	3.75	3.91	G	2.65	3.14	P

*Quality of concrete as a function of UPV: (including; excellent (E) good (G), medium (M) and poor (P))

fraction of fibers. Additionally, Fig. 9(e) shows that for the specimens without any fiber, using RRB fine aggregate as a natural fine aggregate replacement reduces the slope of the weight loss-compressive strength loss relationship.

3.4 Ultrasonic pulse velocity

The ultrasonic pulse velocity (UPV) test is a nondestructive test employed to identify concrete imperfections including nonhomogeneities and cracks throughout the concrete volume, and it can generally be said that higher UPV values are observed in higher quality concretes. Since UPV is a function of the volumetric concentrations of constituents (Albano *et al.* 2009), its lower values can be a sign of a smaller solid phase and volume of cementitious products, as well as more pores and greater distances among particles. In concrete specimens reinforced with fibers, improper mixing or the excessive length of the fibers can be factors contributing to the appearance of these distances, which lead to a lower UPV.

The average UPV values obtained for the three specimens of each concrete mix made with RRB or natural fine aggregate and containing St, FF, PP, and PVA fibers are given in Fig. 10 and Table 6. In addition, the COVs of the UPV values of all the specimens are provided in Table 6. According to the concrete quality classification (based on UPV) provided in the IS 13311-1 standard, four levels including Excellent (E), Good (G), Medium (M), and Poor (P) are defined, for which the UPV ranges expressed in km/s are >4.5, 3.5-4.5, 3.0-3.5, and <3, respectively. Based on this classification, the quality of each concrete mix with respect to the UPV value at different temperatures is reported in Table 6.

Regarding the experimental results at ambient temperature, using 100% RRB fine aggregate compared

with using natural fine aggregate for preparing concrete without any fiber led to a 2.7% increase in the UPV value, which indicates a better quality of the concrete containing RRB fine aggregate. To conduct a comparison between the effects of applying the two fine aggregate types, the UPV ranges can be examined. In this regard, regarding Table 6, the UPV values at ambient temperature for the specimens containing natural fine aggregate change in the range 3.95-4.18 km/s and for the specimens containing RRB fine aggregate, they change in the range 3.72-4.23 km/s. According to the table, the average of the UPV values for the group containing natural fine aggregate (average of 9 mixes) and that of the group containing RRB fine aggregate (average of 9 mixes) are almost the same and equal to 4.06 km/s, and also, the best mixing quality belongs to the FF0.50-R mix with the UPV of 4.23 km/s. By scrutinizing and comparing the UPV results of Plain-N and Plain-R, it can be found that the RRB aggregate improves the UPV values of concrete; however, for the mixes with 0.25% FF fibers, 0.5% PP fibers, and 0.5% PVA fibers, the UPV values for the N-type mixes are higher than those of R-type mixes. This may be the result of the heterogeneous fiber distribution for the three groups of fibers due to the complex shape and hybrid configuration of forta-ferro, the high volume fraction of PP and PVA (0.5% is the maximum fiber volume fraction in most research in the literature), and the different conditions governing the experimental works. Nevertheless, there is an insignificant difference between the results of N-type mixes and R-type mixes for all mixes at room temperature. This trend can be also seen for most of the mixes containing FF, PP and PVA fibers at 400°C; however, the RRB aggregates improve the UPV values for all concrete mixes at 800°C, after the melting and complete removal of the fibers.

Fig. 10 shows the effect of the fiber type and volume

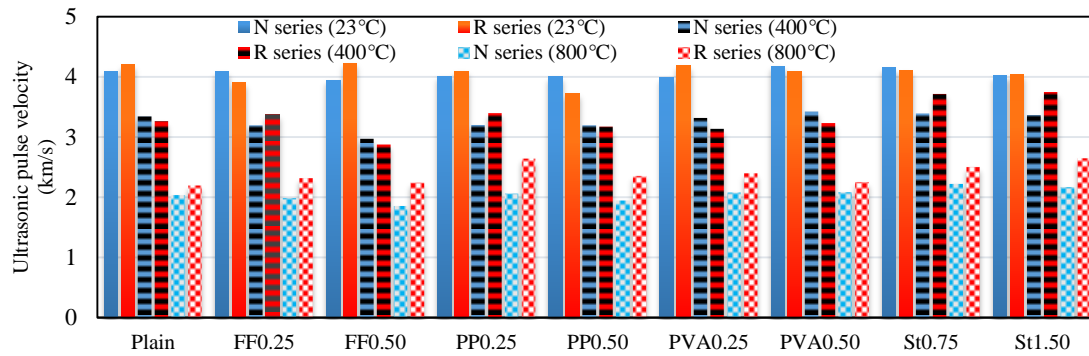


Fig. 10 Ultrasonic pulse velocity of mixtures exposed to elevated temperatures

fraction in the concrete mixes on the UPV. According to the given results, at ambient temperature, employing the FF fibers at the volume fraction of 0.5% in comparison with their 0.25% volume fraction for the mix containing natural fine aggregate leads to a 3.4% reduction of the UPV, while using the higher volume fraction of fibers in the mixes containing RRB fine aggregate increased the UPV values by 8.2%, suggesting a better quality and homogeneity of the concrete. Furthermore, using different volume fractions of PP fibers for the mixes with natural fine aggregate leads to a similar performance; however, regarding the mixes with RRB fine aggregate, as the volume fraction of PP fibers increases, the UPV experiences a 9.27% decrease, which can be a consequence of an inadequate dispersion of fibers throughout the concrete mix, leading to its lower quality. When using PVA and St fibers in the mixes containing RRB fine aggregate, with increasing volume fraction of fibers the UPV decreased, as was the case for the PP fibers, with the UPV reduction values for the PVA and St fibers being 2.4 and 1.7%, respectively. However, in the mixes containing natural fine aggregate, as the content of PVA fibers increased, so did the UPV value, contrary to what was the case for the St fibers.

As the temperature increased to 400°C, the UPV values of all the concrete mixes decreased, indicating increased porosity and decreased density after exposure to the temperature of 400°C. At this temperature, using 100% RRB fine aggregate as a natural fine aggregate replacement for producing concrete without any fiber gave a 2.4% reduction in the UPV, and also, in comparison with ambient temperature, UPV reduction for the specimen without fibers and containing RRB or natural fine aggregate was 18.3 and 22.3%, respectively, indicating that by increasing the temperature to 400°C, the mix without any fiber with RRB fine aggregate showed a porosity increase greater than that of the specimen containing natural fine aggregate. As a comparison between the application of the two types of fine aggregate, the UPV variation range at this temperature for the group of specimens containing natural fine aggregate was 2.97-3.42 km/s, while this range for the group containing RRB fine aggregate was 2.88-3.75 km/s. With regard to Table 6, it is revealed that the average UPV value for the group containing natural fine aggregate (average of 9 mixes) and that for the group containing RRB fine aggregate (average of 9 mixes) are 3.27 and 3.32 km/s, respectively, and also, the best mix quality pertains to the

St1.50-R mix with the UPV of 3.75 km/s.

In addition, as can also be seen in Fig. 10, at 400°C, adding the FF fibers at the volume fraction of 0.5% in the mixes containing natural fine aggregate and those with RRB fine aggregate leads to a 7.2 and 14.5% reduction in the UPV values in comparison with those of the volume fraction of 0.25%. Considering the discussion provided in the next section (Visual Inspection), the higher volume fraction of FF fibers at this temperature results in a higher porosity.

Furthermore, the effects of using different volume fractions of PP fibers in the mixes containing natural fine aggregate are similar to each other at 400 °C, as was the case for ambient temperature; however, regarding the mixes containing RRB fine aggregate, as the content of PP fibers increases, the UPV shows a 6.8% reduction. Contrary to the case for PP fibers, as the contents of PVA and St fibers increase in the mixes containing RRB fine aggregate, the average UPV values increase relative to those of the lower volume contents, with the increase values of 2.9 and 0.8% for the PVA and St fibers, respectively; however, the higher PVA fiber content leads to a higher UPV value in the mixes containing natural fine aggregate, as opposed to the case for St fibers.

As the temperature increased up to 800°C, the UPV values of all the concrete mixes further decreased, and contrary to the other temperatures, at this one being the highest temperature limit applied to the specimens, the UPV values for all the concrete mixes containing RRB fine aggregate were above the corresponding values of the specimens containing natural fine aggregate; the fact that is due to the formation of ceramic bonds among the particles of RRB fine aggregate at this temperature (Baradaran-Nasiri and Nematzadeh 2017). The UPV variations at this temperature for all the specimens containing natural fine aggregate were in the range 1.86-2.22 km/s, while for all the specimens containing RRB fine aggregate, they were in the range 2.19-2.65 km/s. With regard to Table 6, it is revealed that the average UPV value for the group containing natural fine aggregate (average of 9 mixes) and the one containing RRB fine aggregate (average of 9 mixes) is 2.05 and 2.40 km/s, respectively. Moreover, the best mix quality belongs to the St1.50-R mix with the UPV of 2.65 km/s.

Note that the average loss of the UPV value (average of 9 mixes) at 800°C relative to that at ambient temperature

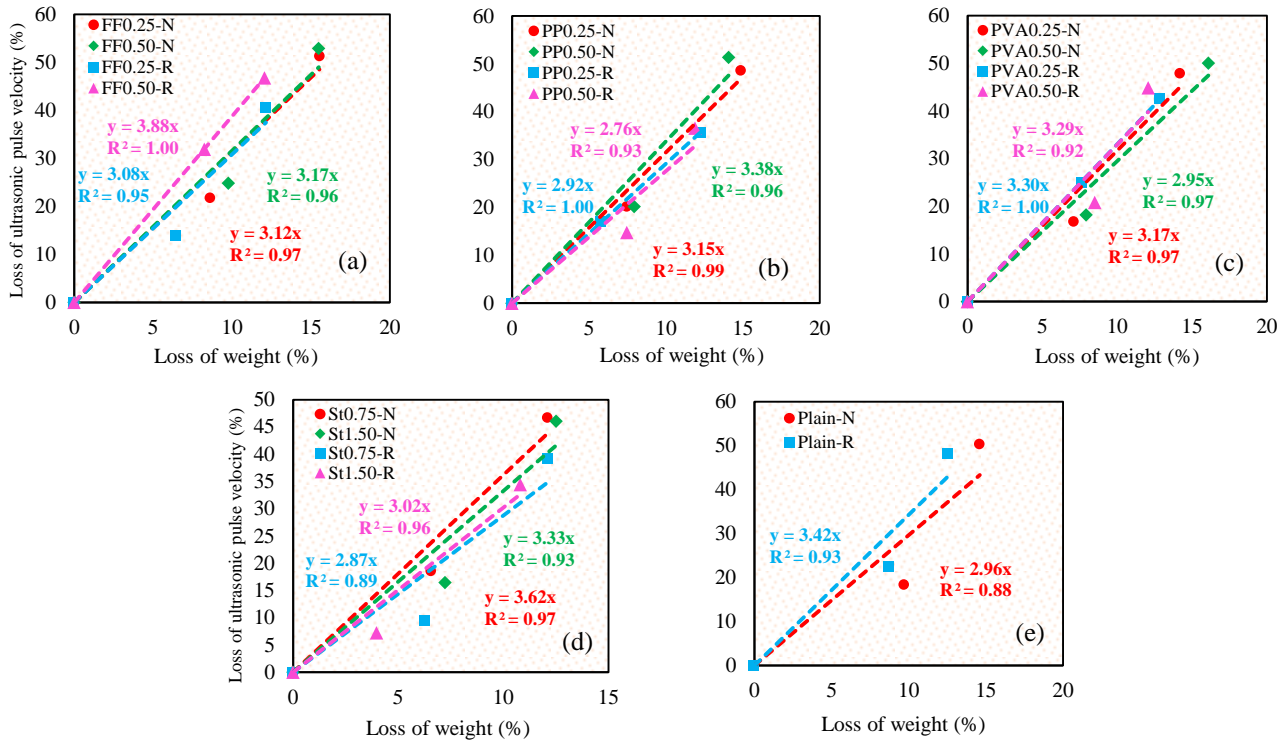


Fig. 11 Relationships between weight loss and ultrasonic pulse velocity loss of mixtures; (a) forta-ferro, (b) polypropylene, (c) polyvinyl alcohol, (d) steel fibers, and (e) plain

for the specimens containing natural and RRB fine aggregates is 49.4 and 41.1%, respectively, which leads the general conclusion that the application of RRB fine aggregate instead of natural fine aggregate gives higher UPV values and a better quality of concrete, particularly at 800°C.

Furthermore, based on Fig. 10 and Table 6, at 800°C, adding the higher volume fractions of the FF, PP, or St fibers in the mixes containing natural fine aggregate led to reduced UPV values for all the cases by 6.5, 5.3, and 2.3%, respectively, and only for the PVA fibers, a slight increase was observed. In addition, using the higher volume fractions of FF, PP, or PVA fibers in the mixes containing RRB fine aggregate decreased the UPV values for all the cases by 3.0, 10.6, and 6.2%, respectively, and the only increase of 6% was achieved by using St fibers. The reason for a higher UPV loss for higher volume contents of polymeric fibers may be due to the fact that more melted fibers escape through the cracks opened within the concrete, leaving more pores behind which in turn exacerbate the UPV loss under elevated temperatures. With respect to Table 6, the COVs of the tested specimens for all the prepared mixes are less than 10% and vary in the range 0.26-8.55%.

3.5 Weight loss-UPV loss relationship

The diagrams shown in Fig. 11 demonstrate the relationships between the weight loss and UPV loss of the concrete mixes. As can be seen, by applying the regression analysis on the experimental results, a linear relationship was established between the weight loss and UPV loss, with

a high coefficient of determination for most concrete mixes. It is seen from the regression lines in Fig. 11 that the percentage of UPV loss of these mixes is in the range of 2.8 to 3.9 times as much as their weight loss percentage. Furthermore, regarding the FF fibers, using the 0.5% volume fraction leads to a small increase in the slope of the weight loss-UPV loss diagram in comparison with using the 0.25% volume fraction for both types of fine aggregates. In addition, the weight loss-UPV loss relationship for either type of fine aggregate shows a different trend from that of the other, as can be seen in Fig. 11(b), such that regarding natural fine aggregate, with increasing content of PP fibers, the relationship slope also increases, while when using RRB fine aggregate, as the content of the fibers increases, the slope of the existing relationship decreases, suggesting a better performance of RRB fine aggregate. It is worth noting that a decreasing slope of the weight loss-UPV loss relationship is considered as the desired behavior, indicating a mix with a higher pulse velocity while losing weight.

Figs. 11(c) and 11(d) demonstrate the weight loss-UPV loss relationships for the PVA and St fibers; according to which, when natural fine aggregate is used, the relationship between weight loss and UPV loss is the same for both fiber types, with a lower relationship slope for a higher fiber content. Moreover, when using RRB fine aggregate, increasing the content of PVA fibers decreases the slope, while increasing the content of St fibers increases the slope. Also, Fig. 11(e) shows that for the specimens without any fiber, using RRB fine aggregate as a natural fine aggregate replacement increases the slope of the weight loss-UPV loss relationship, as previously observed for the weight loss-compressive strength loss relationship.

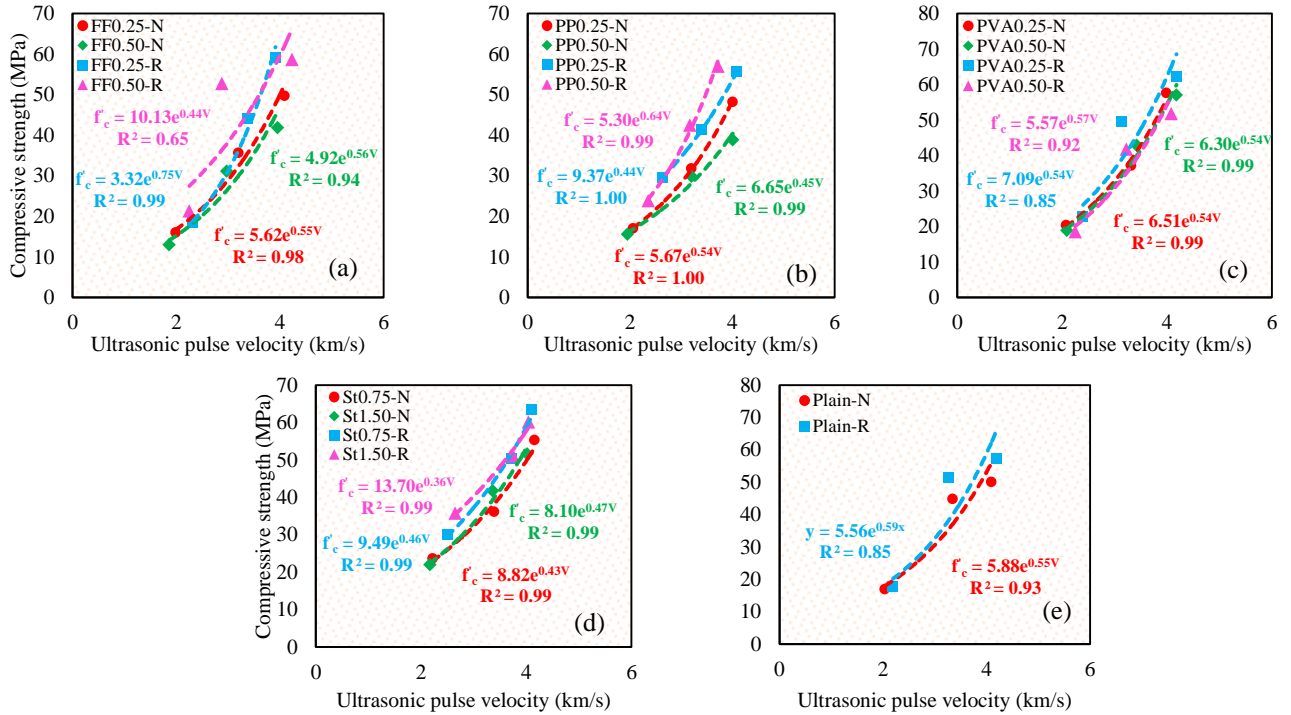


Fig. 12 Empirical relationships between compressive strength and UPV for different mixtures; (a) forta-ferro, (b) polypropylene, (c) polyvinyl alcohol, and (d) steel fibers, and (e) plain

3.6 Compressive strength-UPV relationship

Note that there is no definitive relationship between UPV and compressive strength values which can be applied to determine and measure concrete compressive strength (Nik and Omran 2013). However, considering that the elastic modulus and compressive strength of concrete are related, on one hand, and that the UPV of concrete has a relationship with its elastic modulus and density, on the other, a good incentive to study concrete compressive strength based on its UPV may arise. Many researchers (Nik and Omran 2013, Nematzadeh and Poorhosein 2017, Gül *et al.* 2006) have shown that the compressive strength-UPV relationship can be expressed with the following exponential function

$$f_c' = Ae^{BV} \quad (3)$$

where f_c' and V are the concrete compressive strength and ultrasonic pulse velocity, respectively, and A and B are empirical constants. In this work, by applying the nonlinear regression analysis on the experimental results, appropriate exponential functions were developed for determining the compressive strength-UPV relationship of concrete for each of the mixes containing FF, PP, PVA, and St fibers, as shown in Fig. 12. With respect to their high coefficients of determination (except for FF0.50-R), it can be said that a good relationship exists between the experimental data and regression curves.

Furthermore, by applying the nonlinear regression analysis on the experimental results of all the concrete mixes tested here, a general relationship between compressive strength and UPV was proposed as follows,

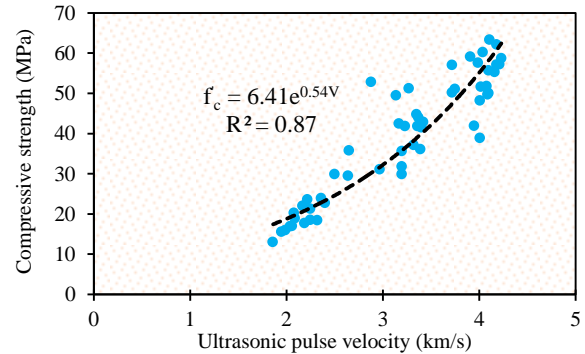


Fig. 13 General empirical relationships between compressive strength and UPV

which demonstrates a good coefficient of determination.

$$f_c' = 6.41e^{0.54V} \quad R^2 = 0.87 \quad (4)$$

Fig. 13 shows the results of the above equation together with the experimental results of this study. The good agreement seen between Eq. (4) and the experimental results indicates that at all temperatures, only by knowing the UPV values, the corresponding compressive strength values can be properly predicted, regardless of the type of fine aggregate as well as the type and content of fibers.

3.7 Visual observation of specimens after exposure to heat

The damage suffered by concrete after exposure to elevated temperatures can be detected by observing its surface. Visual inspections to evaluate the damage of

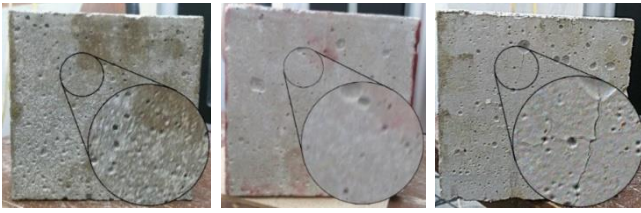


Fig. 14 Surface texture of concrete specimens exposed to elevated temperatures; (a) at 23°C, (b) at 400°C, and (c) at 800°C

concrete exposed to fire usually include controlling for the color change, cracking, and spalling of the surface. Here, concrete specimens were visually observed immediately after removal from the electric furnace, with the obtained results discussed below. Fig. 14 demonstrates concrete surfaces after thermal treatment, and given that no noticeable distinction could be made among the visual inspection results of the specimens containing different fiber types in this study, photos of three concrete specimens were shown in this figure randomly to represent all the specimens in different temperature groups. The surface of the concrete specimens in this work demonstrated no cracks observable by naked eye up to 400°C, due to a good residual compressive strength of the concrete specimens even at 800°C (above 13 MPa for all the groups). Furthermore, as the temperature increased to reach 800°C, some microcracks appeared on the surface of all the specimens, and also, the color of all the specimens changed from the natural concrete color to white, which is attributed to changes in the composition of aggregate grains as well as cement compounds in the mixes.

In the present work, only one exception was observed in the behavior of specimens due to temperature increase, which occurred in the specimens containing FF fibers at 400°C. As can be seen in Fig. 15(a), after removing the specimens containing FF fibers from the furnace, it was observed that all the fibers had been burned and turned black. For other polymeric fibers including the PP and PVA fibers, this phenomenon at this temperature either did not occur or could not be observed due to a very small diameter of these fibers. In addition, as the temperature increased up to 800°C, this behavior could no longer be seen for the mixes containing FF fibers.

Note that most polymeric fibers have a melting point below 200°C, above which, they completely melt and lose their efficiency, particularly in tensile strength. Some researchers (Li *et al.* 2017b, Yu *et al.* 2015) believe that using these fiber types and their consequent melting at elevated temperatures help to reduce the heat-induced pore water pressure of concrete through the pores left behind by these fibers, thus lower concrete deterioration as well as a smaller compressive strength loss relative to those of conventional concrete, is achieved. This subject was also investigated in this study, and as previously discussed, no considerable effect on preventing the compressive strength loss was observed. Fig. 15(b) shows the specimen containing FF fibers (after exposure to 400°C) after the compressive strength test, and from that, it is clear that all the contained fibers have melted, and no sign of surface



Fig. 15 The effect of temperature increase on a specimen containing forta-ferro fibers at 400°C; (a) surface of specimen and (b) specimen after compressive strength test

burn previously seen regarding its outer surface can be observed inside the specimen.

4. Conclusions

This paper presented an experimental program for reusing recycled refractory brick (RRB) fine aggregate as a natural fine aggregate replacement along with the application of steel (St), forta-ferro (FF), polypropylene (PP), and polyvinyl alcohol (PVA) fibers in concrete. Regarding the results obtained here, the following conclusions may be drawn.

- Using 100% RRB fine aggregate as a natural fine aggregate replacement led to an increase of the compressive strength in almost all of the concrete mixes, with the only exception being the PVA0.50 mix for which a decrease was observed.
- The lowest average compressive strength loss (average of the loss results of 4 types of fiber-reinforced concrete mixes prepared for each fiber type) at 400 and 800°C belonged to the St fibers with 22.4 and 38.1%, respectively.
- Considering the compressive strength parameter, using FF fibers at the volume fraction of 0.50% along with RRB fine aggregate resulted in a better thermal performance relative to the volume fraction of 0.25% at all the temperatures, while using these fibers along with natural fine aggregate gave a different trend. In addition, using St fibers in comparison with the other fiber types led to a more improved thermal performance, particularly at 800°C.
- The predictions proposed by the two codes of EN 1994-1-2 and ACI 216 at temperatures below 400 °C are close to the experimental results of the normalized compressive strength of all the mixes containing RRB fine aggregate, while above 550°C, considerable overestimations are shown. Nevertheless, the predictions for the specimens containing natural fine aggregate are more accurate.
- As the temperature increased, weight loss of all the concrete mixes increased. Moreover, at all the temperatures, using 100% RRB fine aggregate replacing natural fine aggregate led to a decreased weight loss of the concrete specimens for most mixes, indicating its positive effect on the concrete integration. Additionally, the best thermal behavior in terms of weight loss was obtained for the mixes containing St fibers.

- As the temperature raised to reach 800°C, the UPV values of all the concrete mixes decreased. In addition, at this temperature, the UPV values for the concrete mixes containing RRB fine aggregate were greater than the corresponding values of those with natural fine aggregate.
- Using the higher volume fraction of the FF, PP, and PVA fibers in the mixes containing RRB fine aggregate at 800°C lowered the UPV values compared with those at the lower volume fractions, while an improvement was obtained by using St fibers.

References

- ACI 228.2R-98 (2004), Nondestructive Test Methods for Evaluation of Concrete in Structures, American Concrete Institute, Farmington Hills, MI.
- ACI Committee 216 (1989), Guide for Determining the Fire Endurance of Concrete Elements (ACI 216R-89), American Concrete Institute, Detroit.
- Afroughsabet, V., Biolzi, L. and Ozbakkaloglu, T. (2016), "High-performance fiber-reinforced concrete: a review", *J. Mater. Sci.*, **51**(14), 6517-6551. <https://doi.org/10.1007/s10853-016-9917-4>.
- Albano, C., Camacho, N., Hernandez, M., Matheus, A. and Gutierrez, A. (2009), "Influence of content and particle size of waste pet bottles on concrete behavior at different w/c ratios", *Waste Manage.*, **29**(10), 2707-2716. <https://doi.org/10.1016/j.wasman.2009.05.007>.
- Aliabdo, A.A., Abd-Elmoaty, A.E.M. and Hassan, H.H. (2014), "Utilization of crushed clay brick in concrete industry", *Alex. Eng. J.*, **53**(1), 151-168. <https://doi.org/10.1016/j.aej.2013.12.003>.
- Arioz, O. (2007), "Effects of elevated temperatures on properties of concrete", *Fire Saf. J.*, **42**(8), 516-522. <https://doi.org/10.1016/j.firesaf.2007.01.003>.
- ASTM C143/C143M (2003), Standard Test Method for Slump of Hydraulic-Cement Concrete, Annual Book of ASTM Standard 04.
- ASTM C150 (2003), Standard Specification for Portland Cement, Annual Book of ASTM Standard 04.
- ASTM C192/C192M (2002), Standard Practice for Making and Curing Concrete Test Specimens in the Laboratory, Annual Book of ASTM Standard 04.
- ASTM C33 (2003), Standard Specification for Concrete Aggregates, Annual book of ASTM standard 04.
- ASTM C494 (2016), Standard Specification for Chemical Admixtures for Concrete, American Society for Testing and Materials International, United States.
- ASTM C597 (2016), Standard Test Method for Pulse Velocity Through Concrete, American Society for Testing Materials International, United States.
- Banthia, N. and Gupta, R. (2004), "Hybrid fiber reinforced concrete (HyFRC): fiber synergy in high strength matrices", *Mater. Struct.*, **37**(10), 707-716. <https://doi.org/10.1007/BF02480516>.
- Baradaran-Nasiri, A. and Nematzadeh, M. (2017), "The effect of elevated temperatures on the mechanical properties of concrete with fine recycled refractory brick aggregate and aluminate cement", *Constr. Build. Mater.*, **147**, 865-875. <https://doi.org/10.1016/j.conbuildmat.2017.04.138>.
- BS 1881-116 (1983), Testing Concretes, Method for Determination of Compressive Strength of Concrete Cubes.
- Buratti, N., Mazzotti, C. and Savoia, M. (2011), "Post-cracking behaviour of steel and macro-synthetic fibre-reinforced concretes", *Constr. Build. Mater.*, **25**(5), 2713-2722. <https://doi.org/10.1016/j.conbuildmat.2010.12.022>.
- Chen, G.M., He, Y.H., Yang, H., Chen, J.F. and Guo, Y.C. (2014), "Compressive behavior of steel fiber reinforced recycled aggregate concrete after exposure to elevated temperatures", *Constr. Build. Mater.*, **71**, 1-15. <https://doi.org/10.1016/j.conbuildmat.2014.08.012>.
- Choumanidis, D., Badogiannis, E., Nomikos, P. and Sofianos, A. (2016), "The effect of different fibres on the flexural behaviour of concrete exposed to normal and elevated temperatures", *Constr. Build. Mater.*, **129**, 266-277. <https://doi.org/10.1016/j.conbuildmat.2016.10.089>.
- Cree, D., Green, M. and Noumowé, A. (2013), "Residual strength of concrete containing recycled materials after exposure to fire: a review", *Constr. Build. Mater.*, **45**, 208-223. <https://doi.org/10.1016/j.conbuildmat.2013.04.005>.
- Domski, J., Katzer, J., Zakrzewski, M. and Ponikiewski, T. (2017), "Comparison of the mechanical characteristics of engineered and waste steel fiber used as reinforcement for concrete", *J. Clean. Prod.*, **158**, 18-28. <https://doi.org/10.1016/j.jclepro.2017.04.165>.
- Eurocode 4 (2004), EN 1994-1-2:2004, Design of Composite Steel and Concrete Structures-Part 1-2: General Rules for Structural Fire Design.
- Ghahremannejad, M., Mahdavi, M., Saleh, A.E., Abhaee, S. and Abolmaali, A. (2018), "Experimental investigation and identification of single and multiple cracks in synthetic fiber concrete beams", *Case Stud. Constr. Mater.*, **9**, e00182. <https://doi.org/10.1016/j.cscm.2018.e00182>.
- Grünwald, S. and Walraven, J.C. (2001), "Parameter-study on the influence of steel fibers and coarse aggregate content on the fresh properties of self-compacting concrete", *Cement Concrete Res.*, **31**(12), 1793-1798. [https://doi.org/10.1016/S0008-8846\(01\)00555-5](https://doi.org/10.1016/S0008-8846(01)00555-5).
- Gül, R., Demirboğa, R. and Güvercin, T. (2006), "Compressive strength and ultrasound pulse velocity of mineral admixed mortars", *IJEMS*, **13**(1).
- Güneyisi, E., Gesoglu, M., Özturan, T. and İpek, S. (2015), "Fracture behavior and mechanical properties of concrete with artificial lightweight aggregate and steel fiber", *Constr. Build. Mater.*, **84**, 156-168. <https://doi.org/10.1016/j.conbuildmat.2015.03.054>.
- Halicka, A., Ogrodnik, P. and Zegardlo, B. (2013), "Using ceramic sanitary ware waste as concrete aggregate", *Constr. Build. Mater.*, **48**, 295-305. <https://doi.org/10.1016/j.conbuildmat.2013.06.063>.
- Hansen, T.C. (2004), *Recycling of Demolished Concrete and Masonry*, CRC Press.
- Hsieh, M., Tu, C. and Song, P. S. (2008), "Mechanical properties of polypropylene hybrid fiber-reinforced concrete", *Mater. Sci. Eng.: A*, **494**(1), 153-157. <https://doi.org/10.1016/j.msea.2008.05.037>.
- IS 13311-1 (1992), Non-Destructive Testing of Concrete-Methods of Tests, Bureau of Indian Standard, New Delhi, India.
- Khalaf, F.M. and DeVenny, A.S. (2004), "Recycling of demolished masonry rubble as coarse aggregate in concrete", *J. Mater. Civil Eng.*, **16**(4), 331-340. [https://doi.org/10.1061/\(ASCE\)0899-1561\(2004\)16:4\(331\)](https://doi.org/10.1061/(ASCE)0899-1561(2004)16:4(331)).
- Khalaf, F.M. and DeVenny, A.S. (2005), "Properties of new and recycled clay brick aggregates for use in concrete", *J. Mater. Civil Eng.*, **17**(4), 456-464. [https://doi.org/10.1061/\(ASCE\)0899-1561\(2005\)17:4\(456\)](https://doi.org/10.1061/(ASCE)0899-1561(2005)17:4(456)).
- Li, X., Bao, Y., Wu, L., Yan, Q., Ma, H., Chen, G. and Zhang, H. (2017b), "Thermal and mechanical properties of high-performance fiber-reinforced cementitious composites after exposure to high temperatures", *Constr. Build. Mater.*, **157**, 829-838. <https://doi.org/10.1016/j.conbuildmat.2017.09.125>.

- Li, X., Bao, Y., Xue, N. and Chen, G. (2017a), "Bond strength of steel bars embedded in high-performance fiber-reinforced cementitious composite before and after exposure to elevated temperatures", *Fire Saf. J.*, **92**, 98-106. <https://doi.org/10.1016/j.firesaf.2017.06.006>.
- Liu, Y., Wang, W., Chen, Y.F. and Ji, H. (2016), "Residual stress-strain relationship for thermal insulation concrete with recycled aggregate after high temperature exposure", *Constr. Build. Mater.*, **129**, 37-47. <https://doi.org/10.1016/j.conbuildmat.2016.11.006>.
- Meng, W. and Khayat, K.H. (2018), "Effect of hybrid fibers on fresh properties, mechanical properties, and autogenous shrinkage of cost-effective UHPC", *J. Mater. Civil Eng.*, **30**(4), 04018030. [https://doi.org/10.1061/\(ASCE\)MT.1943-5533.0002212](https://doi.org/10.1061/(ASCE)MT.1943-5533.0002212).
- Mohammadhosseini, H. and Yatim, J. M. (2017), "Microstructure and residual properties of green concrete composites incorporating waste carpet fibers and palm oil fuel ash at elevated temperatures", *J. Clean. Prod.*, **144**, 8-21. <https://doi.org/10.1016/j.jclepro.2016.12.168>.
- Mohammadhosseini, H., Lim, N.H.A.S., Sam, A.R.M. and Samadi, M. (2018), "Effects of elevated temperatures on residual properties of concrete reinforced with waste polypropylene carpet fibres", *Arab. J. Sci. Eng.*, **43**(4), 1673-1686. <https://doi.org/10.1007/s13369-017-2681-1>.
- Nematzadeh, M. and Baradaran-Nasiri, A. (2018), "Residual properties of concrete containing recycled refractory brick aggregate at elevated temperatures", *J. Mater. Civil Eng.*, **30**(1), 04017255. [https://doi.org/10.1061/\(ASCE\)MT.1943-5533.0002125](https://doi.org/10.1061/(ASCE)MT.1943-5533.0002125).
- Nematzadeh, M. and Fallah-Valukolaee, S. (2017a), "Effectiveness of fibers and binders in high-strength concrete under chemical corrosion", *Struct. Eng. Mech.*, **64**(2), 243-257. <https://doi.org/10.12989/sem.2017.64.2.243>.
- Nematzadeh, M. and Fallah-Valukolaee, S. (2017b), "Erosion resistance of high-strength concrete containing forta-ferro fibers against sulfuric acid attack with an optimum design", *Constr. Build. Mater.*, **154**, 675-686. <https://doi.org/10.1016/j.conbuildmat.2017.07.180>.
- Nematzadeh, M. and Hasan-Nattaj, F. (2017), "Compressive stress-strain model for high-strength concrete reinforced with Forta-Ferro and steel fibers", *J. Mater. Civil Eng.*, **29**(10), 04017152. [https://doi.org/10.1061/\(ASCE\)MT.1943-5533.0001990](https://doi.org/10.1061/(ASCE)MT.1943-5533.0001990).
- Nematzadeh, M. and Poorhosein, R. (2017), "Estimating properties of reactive powder concrete containing hybrid fibers using UPV", *Comput. Concrete*, **20**(4), 491-502. <https://doi.org/10.12989/cac.2017.20.4.491>.
- Nik, A.S. and Omran, O.L. (2013), "Estimation of compressive strength of self-compacted concrete with fibers consisting nano-SiO₂ using ultrasonic pulse velocity", *Constr. Build. Mater.*, **44**, 654-662. <https://doi.org/10.1016/j.conbuildmat.2013.03.082>.
- Peng, G.F., Yang, W.W., Zhao, J., Liu, Y.F., Bian, S.H. and Zhao, L.H. (2006), "Explosive spalling and residual mechanical properties of fiber-toughened high-performance concrete subjected to high temperatures", *Cement Concrete Res.*, **36**(4), 723-727. <https://doi.org/10.1016/j.cemconres.2005.12.014>.
- Poorhosein, R. and Nematzadeh, M. (2018), "Mechanical behavior of hybrid steel-PVA fibers reinforced reactive powder concrete", *Comput. Concrete*, **21**(2), 167-179. <https://doi.org/10.12989/cac.2018.21.2.167>.
- Qian, C.X. and Stroeven, P. (2000), "Development of hybrid polypropylene-steel fibre-reinforced concrete", *Cement Concrete Res.*, **30**(1), 63-69. [https://doi.org/10.1016/S0008-8846\(99\)00202-1](https://doi.org/10.1016/S0008-8846(99)00202-1).
- Sagoe-Crentsil, K.K., Brown, T. and Taylor, A.H. (2001), "Performance of concrete made with commercially produced coarse recycled concrete aggregate", *Cement Concrete Res.*, **31**(5), 707-712. [https://doi.org/10.1016/S0008-8846\(00\)00476-2](https://doi.org/10.1016/S0008-8846(00)00476-2).
- Sarhat, S.R. and Sherwood, E.G. (2012), "Residual mechanical response of recycled aggregate concrete after exposure to elevated temperatures", *J. Mater. Civil Eng.*, **25**(11), 1721-1730. [https://doi.org/10.1061/\(ASCE\)MT.1943-5533.0000719](https://doi.org/10.1061/(ASCE)MT.1943-5533.0000719).
- Soroushian, P. and Bayasi, Z. (1991), "Fiber type effects on the performance of steel fiber reinforced concrete", *Mater. J.*, **88**(2), 129-134.
- Wijayasundara, M., Mendis, P. and Crawford, R. H. (2018), "Integrated assessment of the use of recycled concrete aggregate replacing natural aggregate in structural concrete", *J. Clean. Prod.*, **174**, 591-604. <https://doi.org/10.1016/j.jclepro.2017.10.301>.
- Xiao, J., Li, J. and Zhang, C. (2005), "Mechanical properties of recycled aggregate concrete under uniaxial loading", *Cement Concrete Res.*, **35**(6), 1187-1194. <https://doi.org/10.1016/j.cemconres.2004.09.020>.
- Yao, W., Li, J. and Wu, K. (2003), "Mechanical properties of hybrid fiber-reinforced concrete at low fiber volume fraction", *Cement Concrete Res.*, **33**(1), 27-30. [https://doi.org/10.1016/S0008-8846\(02\)00913-4](https://doi.org/10.1016/S0008-8846(02)00913-4).
- Yazıcı, Ş., İnan, G. and Tabak, V. (2007), "Effect of aspect ratio and volume fraction of steel fiber on the mechanical properties of SFRC", *Constr. Build. Mater.*, **21**(6), 1250-1253. <https://doi.org/10.1016/j.conbuildmat.2006.05.025>.
- Yu, K.Q., Dai, J.G., Lu, Z.D. and Leung, C.K. (2015), "Mechanical properties of engineered cementitious composites subjected to elevated temperatures", *J. Mater. Civil Eng.*, **27**(10), 04014268. [https://doi.org/10.1061/\(ASCE\)MT.1943-5533.0001241](https://doi.org/10.1061/(ASCE)MT.1943-5533.0001241).

CC